A Quasi-Steady-State Lap Time Simulation for Electrified Race Cars

Alexander Heilmeier*, Maximilian Geisslinger*, Johannes Betz*

*Chair of Automotive Technology
Technical University of Munich
Garching, Germany
Email: alexander.heilmeier@tum.de

Abstract—In motorsports, lap time simulation (LTS) is used by race engineers to evaluate the effects of setup changes on lap time and energy consumption. Many of the LTS published to date are no longer able to meet today's requirements because more and more racing series are introducing hybrid systems to improve powertrain efficiency. In addition, some racing series have purely electric powertrains. As a result, new types of LTS are needed that can represent the current state of technology. In addition to various powertrain types and topologies, this also includes the drag reduction system as well as the simulation of energy management strategies that control the distribution of energy within the hybrid system. For use as a co-simulation together with a race simulation, yellow flags and pit lanes should also be modeled. This paper presents an LTS that covers these aspects and, thanks to an improved quasi-steady-state solver, delivers accurate results within a short computing time. Particular emphasis was placed on easy parametrization, based on publicly available data. Exemplary results are shown for Formula 1 and Formula E cars on different racetracks. Three different energy management strategies are compared with regard to the most efficient use of the available energy.

Keywords—*quasi-steady-state; lap time simulation; race car; hybrid powertrain; electric powertrain.*

I. Introduction

Motorsport has always served as a technology demonstration for automobile manufacturers. This continues to be the case during the transition from internal combustion engines (ICE) to electric motors. In 2014, the FIA Formula 1 (F1) introduced a hybrid system supporting a 1.6-litre ICE. With this, the system reached a total thermal efficiency of over 50% [1]. In the same year, the first racing series with a purely electric powertrain, the FIA Formula E (FE), started. Today, several racing series use either hybrid systems or even electric motors alone in their powertrains.

Regardless of the racing series, a racing team needs various simulation tools to successfully participate in a race. One of them is a lap time simulation (LTS). It simulates a single race car with a specific setup for one lap on a given racetrack. LTS outputs are not limited to the calculation of lap time, but also focus on further results, such as energy consumption. It can be utilized for virtual setup optimization, for example. In the case of hybrid or purely electrically powered race cars, further requirements exist. Hereby it is important to be able to simulate the effects of different energy management strategies on lap time and energy consumption in order to find the optimal balance. Long-term effects, such as tire wear or fuel mass loss, are usually omitted in the LTS. This is in contrast to race simulations that simulate an entire race and are used to determine the race strategy [2]. However, both types of simulation work closely together because the LTS provides many of the required parameters for a race simulation, such as the lap time mass sensitivity. Therefore, the use as a co-simulation together with a race simulation is another application case.

II. Related Work

In general, LTS can be divided into two groups. The first group calculates a velocity profile for a given raceline. This can be done using a driver model or under the assumption of a perfect driver. Depending on the model implementation, the group can be further classified into steady-state and quasi-steady-state approaches. The second group simultaneously optimizes the raceline and the velocity profile on a given racetrack with a specific target, e.g. to achieve a minimum lap time or to find the most efficient energy management strategy. These problems are usually solved by applying optimal control techniques to transient simulation models. Steady-state, quasi-steady-state and transient simulations are differentiated by their different approaches to the compromise

between accuracy and computational speed. For a more detailed description and differentiation of the three types, we refer to Siegler et al. [3] and Völkl [4].

Siegler et al. [3] compare the three model types. They find that quasi-steady-state and transient approaches deliver more accurate results than the steady-state modeling. Further research is carried out for a quasi-steady-state approach using a g-g-v diagram calculated by optimal control techniques in Brayshaw et al. [5]. The results show that it has a similar sensitivity to setup changes as an optimized transient solution of a seven-degrees-of-freedom (7DOF) model. Colunga et al. [6] published a method to transform the differential equations of a 7DOF suspension and a transient cornering model into a discrete state-space representation. The approach can be used to evaluate the impact of road roughness, for example. Coming to pure optimal control techniques with transient models, Casanova [7] and Kelly [8] are representatives for the minimum lap time target. The latter improves robustness of the solution in terms of driveability by considering stability criteria in the optimization problem. He also finds that a quasi-steady-state model provides comparable results to a transient model if it is applicable. However, both publications have large computation times of several hours for simulating a single lap. A methodology for the integration of transient modeling into the quasi-steady-state calculation method is presented by Völkl [4]. The transient states are computed in a separate model and solved iteratively by superposition. Timings et al. [9] show an LTS based on model predictive control and extended by a compensatory controller for robustness to driver mistakes and disturbances. Therefore, the calculated lap time is more likely to be achieved in reality. The related publications Perantoni et al. [10] and Limebeer et al. [11] minimize lap time utilizing a 3D-representation of the racetrack. A method to compute the time-optimal energy management strategy for the F1 hybrid powertrain is described by Limebeer et al. [12]. Ebbesen et al. [13] present an approach that leads to a quick solving of the optimal control problem for this case, but results in lower accuracy. However, treating the energy management as an optimization problem does not necessarily deliver driving behavior strategies that are feasible during a race.

III. Methodology

Our target was to develop a lap time simulation that is suitable for use as a co-simulation together with a race simulation. In the future, the tandem could be utilized to determine and adapt the race strategy of an autonomous race car online during the race, e.g. in the racing series Roborace [14], [15]. Therefore, a low computation time and robust convergence characteristics were important demands for the solver. Furthermore it should be adjustable to different racing series and reflect the current state of technology. Accordingly, it should provide options for simulating the drag reduction system (DRS) as well as the powertrain topologies rear-wheel drive (RWD), front-wheel drive (FWD) and all-wheel drive (AWD). The same applies to the powertrain types (pure ICE, hybrid system and pure electric motors), including the corresponding energy management strategies. In addition, external influences on the lap time, such as yellow flags or driving through the pit, should also be taken into account. The research on literature shows that there is no LTS fulfilling the stated demands.

Our LTS consists of three parts: racetrack model, vehicle model and solver. Since we do not have access to any team data, the simulation is designed in such a way that it can be parametrized based on publicly available data, such as onboard video streams and lap times. It can be utilized for almost every (circuit) racing series. For this paper, we have focused on F1 because it is the most popular racing series and includes a hybrid powertrain that allows us to analyze and compare different energy management strategies. This section presents the most important aspects of the three parts.

A. Racetrack model

The main purpose of the racetrack model is to provide the curvature profile of the racetrack for the solver. The starting point for this is GPS coordinates of the centerline of the racetrack, which can be obtained from the OpenStreetMap project [16], for example. For various types of LTS, the centerline would be a valid input, since the raceline is found together with the velocity profile during execution of the solver. However, this is computationally expensive. Therefore, we want to enter a pre-computed raceline directly. Then, the solver only needs to calculate the exact velocity profile for it. To obtain the raceline on the basis of the centerline, we implemented a path optimization based on a curvature minimization. The minimum curvature line is reasonable near a real raceline, as it allows the highest cornering speeds for a given lateral acceleration limit by the race car. The approach is based on Braghin et al. [17], but has been significantly extended and will be presented in another paper. The raceline of the Shanghai racetrack is shown in Figure 1.
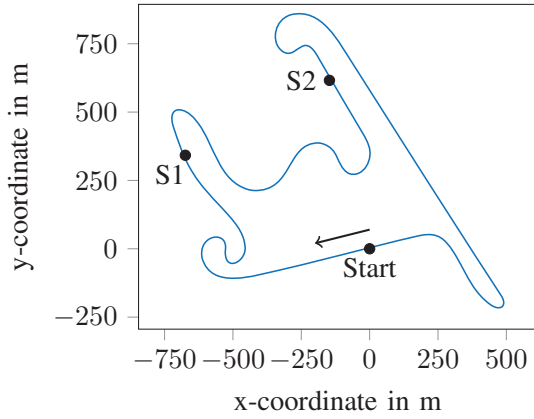
Fig. 1. Raceline of the Shanghai racetrack. S1 and S2 are the boundaries of sector 1 and sector 2. Sector 3 ends at the start/finish line.

Based on the x-y coordinates, the curvature κ_i of the ith raceline point can be calculated by [18, p. 373]

$$\kappa_i = \frac{x_i' y_i'' - y_i' x_i''}{\left(x_i'^2 + y_i'^2 \right)^{\frac{3}{2}}}. \tag{1}$$

The curvature profile for our Shanghai raceline is shown in Figure 2. Due to the previous optimization, it is very smooth. Otherwise, it would have to be processed because it is a decisive factor for the calculated velocity profile and lap time. This can be done by applying a moving average filter, for example.
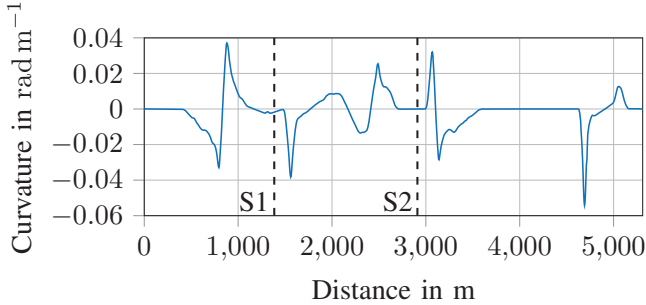

Fig. 2. Curvature profile of the Shanghai raceline. S1 and S2 are the sector boundaries.

For race strategy purposes, it is useful to know how much lap time it costs to drive through the pit with the prescribed speed limit. Furthermore, there is a global speed limit in some racing series, for example in FE. Hence, the racetrack model includes the option to specify a maximum velocity for every discretization point on the raceline.

B. Vehicle model

The vehicle model provides all car-related values to the solver. In order to ensure an easy parametrization, we

kept it simple without neglecting important effects. The basis is a simplified two-track model, which is regarded in steady-state and does not include kinematic relations. All the required parameters are described in Table I.

One central task is to calculate the transmittable tire forces, considering the velocity v and longitudinal and lateral accelerations a_x and a_y. The tire model considers the effect of degressive tire force potential $F_{\text{tire,pot}}$ with rising tire load F_z as well as a friction value μ:

$$F_{\text{tire,pot}} = \mu \left(p_1\, F_z + p_2\, F_z^2 \right). \tag{2}$$

The parameters p_1 and p_2 must be adjusted to the specific tire. The friction value can be used to include the effects of weather or tarmac variation on different racetracks. Longitudinal and lateral tire load transfers, as well as the effect of aerodynamic downforce, are considered within tire load calculation. For the front left tire (FL), we obtain (3). The remaining tire loads are calculated accordingly. The simulated tire load profiles for a F1 car in Shanghai are displayed in Figure 3. It can be used to check for plausibility of the aerodynamic downforce as well as to determine the most stressed tire on a particular track.

$$
\begin{aligned}
F_{z,\text{FL}} = {} & \frac{1}{2}\, m\, g\, \frac{l_{\text{cog,r}}}{l} - \frac{1}{2}\, m\, a_x\, \frac{h_{\text{cog}}}{l} \\
& - m\, a_y\, \frac{l_{\text{cog,r}}}{l}\, \frac{h_{\text{cog}}}{s} + \frac{1}{2}\, \frac{1}{2}\, c_{z,A,f}\, \rho_{\text{air}}\, v^2.
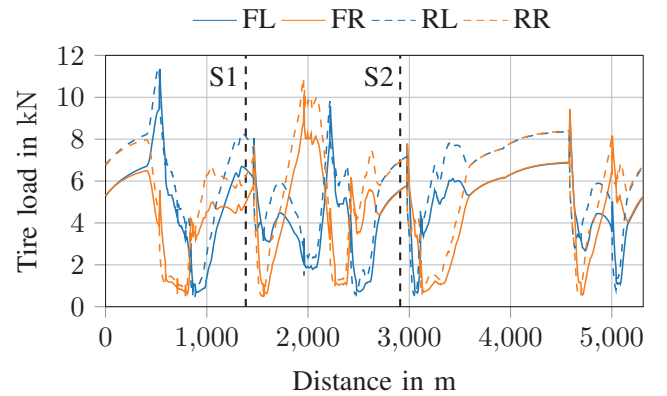\end{aligned} \tag{3}
$$

Fig. 3. Simulated tire loads for a F1 car on the Shanghai racetrack (FL = front left, FR = front right, RL = rear left, RR = rear right). S1 and S2 are the sector boundaries.

As depicted in Figure 4, the F1 powertrain consists of an ICE, an additional electric motor (MGU-K), an electrified turbocharger (MGU-H) and an electric energy storage (ES). Kinetic energy can be recuperated in the MGU-K during braking. The MGU-H can recuperate heat energy from the exhaust gases of the ICE. During acceleration, the recuperated energy can be used in the

MGU-K to provide additional torque ("boosting"). In a 2017 F1 car, the energy flows from ES to MGU-K and back are limited to $4\,\mathrm{MJ/lap}$ or $2\,\mathrm{MJ/lap}$, respectively [19].
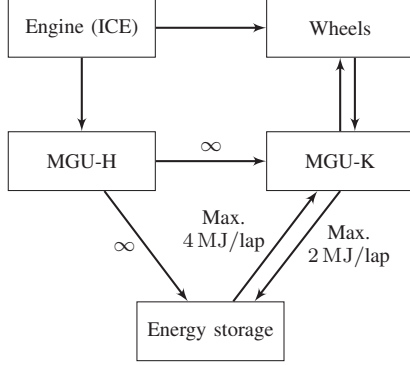

Fig. 4. Powertrain structure and energy flows of a 2017 F1 car.

This powertrain structure is the most general structure in use. It can easily be adapted to the other pure ICE and pure electric motors cases, with the omission of some components. The powertrain topology can be switched between RWD, FWD and AWD and is set to the former for F1 and FE. The power curve of the ICE is modeled by a third-order polynomial. It is fitted based on the maximum power P_{max} acting at n_{max} and the power drop P_{diff} appearing on both sides of the maximum power point at the beginning and end of the primarily used engine speed range n_{begin} and n_{end}. Below 75% of n_{begin}, the power level is kept constant. Figure 5 shows the output of the model.

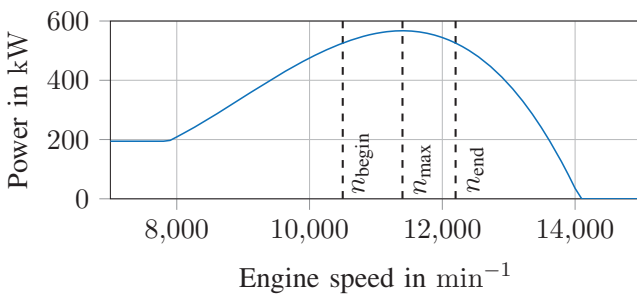
Fig. 5. Modeled power curve of the combustion engine of a 2017 F1 car.

The fuel flow in the ith raceline segment is calculated by

$$b_{\mathrm{e},i} = \sqrt{\frac{P_i}{P_{\mathrm{max}}}}\, b_{\mathrm{e,max}}. \tag{4}$$

The assumptions for this are that the maximum fuel flow $b_{\mathrm{e,max}}$ is reached at P_{max}, and that the efficiency at full power is higher than at partial power. In F1, $b_{\mathrm{e,max}}$ is

limited to $100\,\mathrm{kg\,h^{-1}}$ by the regulations. In the electric parts of the powertrain, the efficiencies $\eta_{\mathrm{MGU\text{-}K,boost}}$ and $\eta_{\mathrm{MGU\text{-}K,re}}$ are considered when boosting (during acceleration) or recuperating (during deceleration) are performed with the MGU-K. Hereby, the MGU-K only acts on the driven axle(s). For the MGU-H, we assume that it recuperates the part $\eta_{\mathrm{MGU\text{-}H,re}}$ of the energy that is supplied by the ICE during every acceleration segment. This happens under the assumption that the power curve of the ICE already includes the influence of the MGU-H.

The torque request is distributed between ICE and MGU-K in such a way that the MGU-K is not used for as long as the ICE can fully provide all of the requested torque at the current engine speed. Otherwise, the MGU-K provides boost if the charging state of the ES is sufficient and the energy management (EM) allows it. Therefore, for every discretization point on the raceline, the EM determines whether boosting should be used based on the underlying strategy. We also implemented a virtual accelerator pedal, which can be utilized to simulate the effect of driving under yellow flag conditions. Yellow flags indicate danger on the track, which is why the drivers have to slow down. As no fixed velocity limit exists, this cannot be considered within the track model.

One important aspect is the inclusion of DRS. Since the 2011 season, the driver can activate DRS under certain conditions to reduce aerodynamic drag on long straights, and thus facilitate overtaking due to the increased maximum velocity. Therefore, the normal drag coefficient $c_{\mathrm{w,A}}$ is replaced by $c_{\mathrm{w,A,DRS}}$ within the DRS zones that are supplied by the track model.

C. Solver

The solver calculates the velocity profile along the raceline with recourse to the vehicle model. The lap time can then be derived from this. Since the LTS should be able to run offline as well as online on a car, the main requirements are accurate results, fast computing time and robust convergence characteristics. For this reason, a quasi-steady-state approach is preferred over steady-state and transient approaches. It considers combined longitudinal and lateral accelerations and different radii for every discretization point, while the vehicle model is still regarded as being in a steady-state [3].

For quasi-steady-state modeling there are two common solver types: "forward/backward" (e.g. [5], [17]) and "pure forward". The former searches for the minimum radius of every corner and then calculates two velocity profiles starting from the maximum possible velocity in this point, one forward and one backward. This is done considering the acceleration capabilities of

the car. The various parts along the raceline are finally intersected. As the name implies, the "pure forward" solver calculates only one velocity profile in forward direction. In every discretization point it tries to brake down to standstill within the next few raceline segments. If this is possible within the acceleration capabilities, it further accelerates, else it decelerates from the previous step. The "forward/backward" solver is faster but not as realistic because it uses "future" and therefore wrong lateral and longitudinal accelerations as well as velocities during the backward steps to calculate the velocities at preceding points. Furthermore, it is very susceptible to noisy curvature profiles, as they make it difficult to determine the apex exactly. By combining the working principles, our improved "forward/backward plus" solver increases accuracy in comparison to "forward/backward" and decreases computing time in comparison to "pure forward". The underlying assumption for a reduction of the computing time is that a much larger part of the lap is accelerated rather than decelerated.

A simplified workflow of the solver is depicted in Figure 6. Starting with a given start velocity, the solver loops through the discretized curvature profile. At each point, it first calculates the acting lateral acceleration a_y for the current velocity. Together with a separately determined estimation of the longitudinal acceleration a_x in the current step, it is then used to calculate the tire loads, cp. (3), and thus the tire force potentials, cp. (2). For the car to be able to stay on track, the lateral acceleration forces $F_{y,f}$ and $F_{y,r}$ calculated by

$$F_{y,f} = m\, a_y\, \frac{l_{\text{cog,r}}}{l} \text{ and}$$
$$F_{y,r} = m\, a_y\, \frac{l_{\text{cog,f}}}{l}$$

(5)

must stay below the according tire force potentials $F_{\text{tire,pot,f}}$ and $F_{\text{tire,pot,r}}$ of the front and rear axle. If this is the case, we stay within the forward loop. Working on the assumption that a race driver always uses the full potential of either the tire or the powertrain, the solver calculates the longitudinal acceleration force F_x as given by

$$F_{\text{tire,remain,f}} = \sqrt{F_{\text{tire,pot,f}}^2 - F_{y,f}^2}\,,$$
$$F_{\text{tire,remain,r}} = \sqrt{F_{\text{tire,pot,r}}^2 - F_{y,r}^2} \text{ and}$$

(6)

$$F_x = \min\left(F_{\text{tire,remain,f/r}},\, F_{\text{powertrain}}\right).$$

(7)

The powertrain topology determines which axles should be considered in (7). (6) comprises that the tire force potential is divided among longitudinal and lateral
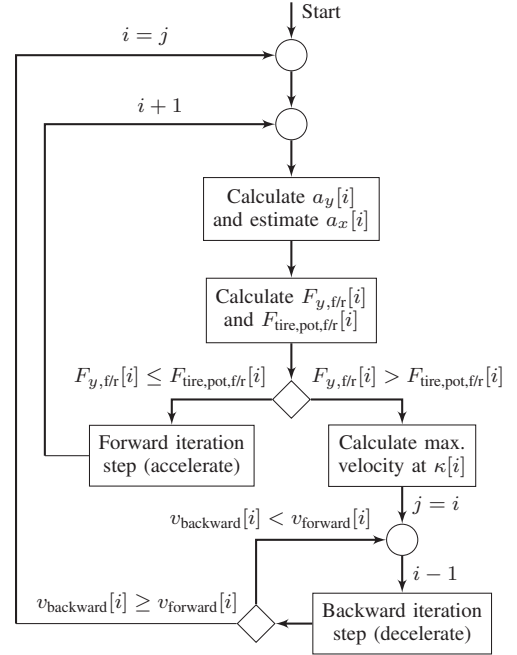

Fig. 6.   Workflow of the "forward/backward plus" solver.

forces, according to the friction circle. F_x is used to obtain the longitudinal acceleration a_x for the upcoming track segment. Together with its step size s_{step}, the new velocity at the next point $i+1$ can be derived by

$$v_{i+1} = \sqrt{v_i^2 + 2\, a_x\, s_{\text{step}}}.$$

(8)

If the potential of one axle is exceeded by the respective lateral force, the car is too fast. In this case, we first calculate the maximum possible velocity at the current curvature κ_i. This is achieved within a separate loop, in which the car accelerates from a low velocity until the full tire potentials are used. The maximum possible velocity cannot be determined directly due to the mutual influence between aerodynamic forces and tire potentials. In longitudinal direction, the driven tires only transmit the force required to overcome drag and rolling resistance as we can assume $a_x = 0\,\text{m s}^{-2}$ at the apex. Afterwards, a temporary backward loop is started, in which the longitudinal deceleration potential of the preceding steps is used. This fully utilizes the tire potentials of both axles, under the assumption of an ideal brake force distribution. In each of these intermediate steps, the velocity as well as the acting longitudinal and lateral acceleration at the preceding point are again approximated in a separate loop. As before, this is necessary because velocity (and therefore aerodynamic downforce), longitudinal and lateral acceleration and tire loads and potentials influence each other. The loop stops as soon as the velocity calculated backward v_{backward} intersects

the originally calculated velocity v_{forward}. Subsequently, the forward loop is resumed at point j that originally caused the backward loop.

The proper start velocity of the lap is initially unknown. A solution for this is to temporarily add a small part of the lap in front of the actual lap. The size of this part must be long enough to ensure that the car decelerates at least once before entering the actual lap to be simulated.

The lap time can be calculated by summing up the time intervals $t_{\text{int},i}$ of every track segment obtained by

$$t_{\text{int},i} = 2\,\frac{s_{\text{step}}}{v_i + v_{i+1}}. \tag{9}$$

Of course, the solver calculates many other variables as well, such as gears, engine speeds or energy consumption in the hybrid powertrain. These calculations are performed in a straightforward manner and are not, therefore, explained in detail here.

D. Parametrization

Some of the vehicle model parameters required can be derived from the technical regulations [19]. For the rest, techniques such as sound analysis and video analysis based on onboard video streams must be used. Velocity and engine speed profiles, as well as the gear choices can be automatically extracted from an onboard video stream by optical character recognition (OCR), for example. This data can also be used to draw further conclusions, such as regarding engine power and gear ratios, for example. The parameters applied for the F1 car in Shanghai can be found in Tables I and II.

IV. RESULTS

The entire simulation is implemented in Python 3 using the numerical math library NumPy. One simulation run for a lap in Shanghai (including the determination of the correct start velocity) takes about $1.3\,\text{s}$ on a laptop computer (Intel i7 2.7 GHz, 16 GB RAM). The raceline with a length of $5{,}310\,\text{m}$ is discretized in steps of $5\,\text{m}$ for this example. In literature, step sizes of $10\,\text{m}$ are often used [8], [13]. This step size, however, leads to a significant deviation in lap times in our simulation. The following paragraphs present the validation of the LTS, as well as some interesting simulation results.

A. Validation

The simulation was validated in terms of velocity profiles obtained from onboard video streams of various qualifying laps of the 2017 season. Figure 7 compares

TABLE I.   OVERVIEW OF THE REQUIRED SIMULATION PARAMETERS WITH EXEMPLARY VALUES OF A 2017 F1 CAR.

Parameter	Description	Example value
General		
m	Mass incl. driver and fuel	$733\,\text{kg}$
l	Wheelbase	$3.6\,\text{m}$
s	Trackwidth	$1.6\,\text{m}$
$l_{\text{cog,r}}$	Distance center of gravity to rear axle	$1.632\,\text{m}$
h_{cog}	Height of center of gravity	$0.335\,\text{m}$
$c_{\text{w,A}}$	Drag coefficient (incl. ref. area)	$1.56\,\text{m}^2$
$c_{\text{w,A,DRS}}$	Drag coefficient (incl. ref. area) (DRS)	$1.295\,\text{m}^2$
$c_{\text{z,A,f}}$	Lift coefficient front (incl. ref. area)	$2.20\,\text{m}^2$
$c_{\text{z,A,r}}$	Lift coefficient rear (incl. ref. area)	$2.68\,\text{m}^2$
ρ_{air}	Air density	$1.18\,\text{kg}\,\text{m}^{-3}$
Engine		
n_{begin}	Engine speed (start of range used)	$10{,}500\,\text{min}^{-1}$
n_{max}	Engine speed (maximum power)	$11{,}400\,\text{min}^{-1}$
n_{end}	Engine speed (end of range used)	$12{,}200\,\text{min}^{-1}$
P_{max}	Maximum power at n_{max}	$567\,\text{kW}$
P_{diff}	Power drop at n_{begin} and n_{end}	$41\,\text{kW}$
$b_{\text{e,max}}$	Maximum fuel flow	$100\,\text{kg}\,\text{h}^{-1}$
$P_{\text{max,MGU-K}}$	Maximum power (MGU-K)	$120\,\text{kW}$
$M_{\text{max,MGU-K}}$	Maximum torque (MGU-K)	$200\,\text{N}\,\text{m}$
$\eta_{\text{MGU-K,boost}}$	Efficiency (MGU-K, boost)	0.9
$\eta_{\text{MGU-K,re}}$	Efficiency (MGU-K, recuperation)	0.15
$\eta_{\text{MGU-H,re}}$	Efficiency (MGU-H)	0.1
$v_{\text{min,MGU-K}}$	Minimum velocity to use MGU-K	$100\,\text{km}\,\text{h}^{-1}$
Gearbox		
i_{trans}	Transmission ratios	0.040
n_{shift}	Shift speeds	$10{,}000\,\text{min}^{-1}$
e_i	Torsional mass factors	1.16
η_{g}	Efficiency of gearbox and transmission	0.96
Tire		
f_{roll}	Rolling resistance	0.03
c_{tire}	Circumference of tire	$2.073\,\text{m}$
$p_{1,\text{f}}$	Tire model parameter	$1.66\,\text{N}^{-1}$
$p_{2,\text{f}}$	Tire model parameter	$-2.5\text{e-}5\,\text{N}^{-2}$
$p_{1,\text{r}}$	Tire model parameter	$2.03\,\text{N}^{-1}$
$p_{2,\text{r}}$	Tire model parameter	$-2.0\text{e-}5\,\text{N}^{-2}$

TABLE II.   GEARBOX SIMULATION PARAMETERS WITH EXEMPLARY VALUES OF A 2017 F1 CAR.

gear	1	2	3	4	5	6	7	8
i_{trans}	0.040	0.070	0.095	0.117	0.143	0.172	0.190	0.206
n_{shift} (min^{-1})	10,000	11,800	11,800	11,800	11,800	11,800	11,800	-
e_i	1.16	1.11	1.09	1.08	1.08	1.08	1.07	1.07

Hamilton's lap in Shanghai to the simulation result. In general, the profiles fit well together, e.g. in term of maximum and minimum velocities. At a distance of $3{,}950\,\text{m}$, reality and simulation show a small kink originating from DRS activation. However, it can be seen that in reality some passages can be passed much faster, e.g. at $2{,}050\,\text{m}$, $2{,}400\,\text{m}$ and $3{,}300\,\text{m}$. This can be explained by different racelines. In reality, drivers often use the curbs in the corners to drive a raceline with a larger radius. Since we do not know the exact track widths including the curbs, such effects are not included in our raceline calculation. Another inaccuracy is that the braking points in the real data are somewhat earlier than in the simulation. The reason for this is the tire model, which currently assumes the same potentials in longitudinal and lateral direction. Further validation including velocity profile, engine

TABLE III.   COMPARISON OF THE SECTOR TIMES OF A F1 CAR
ON THE SHANGHAI RACETRACK.

	Simulation	Reality	Difference
Sector 1	24.437 s	24.036 s	0.401 s
Sector 2	27.222 s	27.079 s	0.143 s
Sector 3	39.847 s	40.563 s	−0.716 s
Lap time	91.506 s	91.678 s	−0.172 s

speed profile, gear choices and energy consumption was carried out against the professional LTS RaceSim [20] showing good correlation.
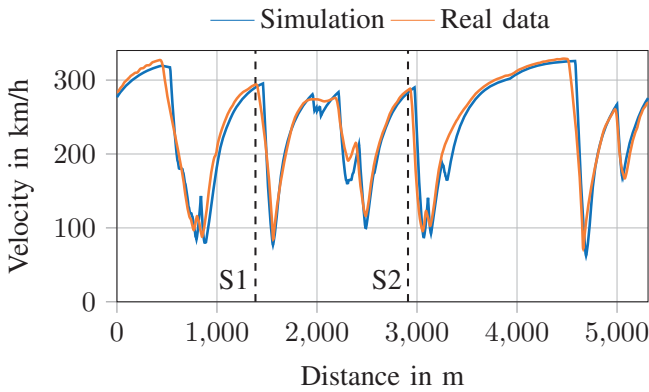

Fig. 7.   Simulated velocity profile for a F1 car in comparison to the real profile of Hamilton's qualifying lap on the Shanghai racetrack. S1 and S2 are the sector boundaries.

For Shanghai, a lap time of $91.506\,\text{s}$ is calculated under qualifying conditions, i.e., DRS is allowed and the car starts with a fully charged ES and applies the MGU-K wherever possible. In reality, Hamilton reached $91.678\,\text{s}$. The small difference shows accurate results can be achieved despite the fact that many parameters are derived from publicly available data. Table III shows that sectors 1 and 3 differ most. In sector 1 it can be traced back to a higher top speed on the straight and a faster passage through the chicane in reality. In sector 3 it is explainable by later braking points at the end of the straights in simulation.

We also simulated the Budapest, Monza and Spielberg racetracks. The aerodynamic coefficients as well as the transmission ratios were therefore slightly adapted to the track characteristics (Monza is a low downforce track while Budapest requires much more downforce) based on information provided by Pirelli [21]. For Monza we furthermore changed the friction value in (2) to $\mu = 0.65$ because the 2017 qualifying was held on a wet track. We found that the qualifying lap times calculated fell within a range of $\pm 1.5\,\text{s}$ of the real results without tuning of other parameters. In conclusion, we can state that the most important aspects have been modeled and a valid parametrization example found. It should be noted,

however, that despite the simple models, the absolute value results depend significantly on the parameters being properly adjusted. Without insight into internal team data, they can only be regarded as reference values. Nevertheless, these values are usually less important than the relative changes between multiple simulation runs with varying inputs to determine whether a setup change was advantageous or disadvantageous, or to obtain a sensitivity, such as the lap time mass sensitivity.

B. Sensitivity analysis for a Formula 1 car

In addition to the velocity profile, a great deal of additional data is output by the LTS, such as the tire loads, engine speeds and charging state of the ES. The simulation is therefore well suited for sensitivity analyses, for instance in order to quantify the influence of vehicle mass on lap time and energy consumption. An example is shown in Figure 8 proving that the relationship between mass and lap time is almost linear when the relevant range from $730\,\text{kg}$ to $830\,\text{kg}$ is considered. The lap time mass sensitivity is $0.062\,\text{s}\,\text{kg}^{-1}$ in this case.
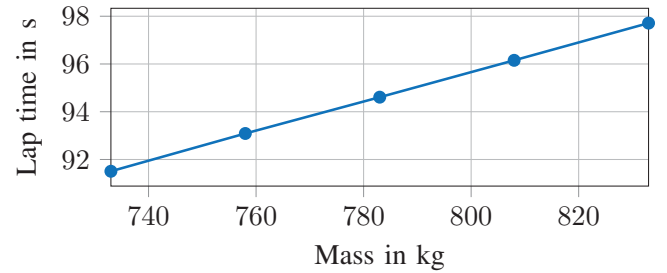

Fig. 8.   Simulated influence of mass on lap time for a F1 car on the Shanghai racetrack.

C. Energy management strategies for a Formula 1 car

Another important aspect is the evaluation of different energy management strategies. The key question is where on the track the MGU-K boost must be used to obtain the biggest lap time advantage from the limited energy available. The energy management strategy can be entered into the simulation by specifying whether or not boosting is allowed for each discretization point. We evaluate three exemplary strategies: "first come, first boost", "longest time to braking point" and "lowest speed". The first one uses the boost as soon as the tires allow it and until the energy is exhausted. The second strategy is based on the idea that the velocity advantage gained by the additional energy is used for as long as possible before braking. "Lowest speed" follows the approach that a given energy input allows a greater speed advantage at low speeds

TABLE IV.   COMPARISON OF DIFFERENT ENERGY
MANAGEMENT STRATEGIES FOR THE F1 HYBRID SYSTEM IN
SHANGHAI WITH A LIMITED AMOUNT OF ELECTRIC ENERGY
AVAILABLE.

Energy management strategy	t_{lap}	Δt_{lap}	m_{fuel}
No boost at all	94.445 s	1.320 s	1.93 kg
First come, first boost	93.602 s	0.477 s	1.90 kg
Longest time to braking point	93.134 s	0.009 s	1.90 kg
Lowest speed	93.125 s	-	1.89 kg

TABLE V.   EXEMPLARY SIMULATION PARAMETERS OF A
2017/2018 FE CAR.

Parameter	Description	Example value
General		
m	Mass incl. driver	880 kg
l	Wheelbase	3.1 m
s	Trackwidth	1.3 m
$l_{cog,r}$	Distance center of gravity to rear axle	1.194 m
h_{cog}	Height of center of gravity	0.345 m
$c_{w,A}$	Drag coefficient (incl. ref. area)	1.15 m^2
$c_{z,A,f}$	Lift coefficient front (incl. ref. area)	1.24 m^2
$c_{z,A,r}$	Lift coefficient rear (incl. ref. area)	1.52 m^2
Engine		
$P_{max,MGU\text{-}K}$	Maximum power (MGU-K)	200 kW
$M_{max,MGU\text{-}K}$	Maximum torque (MGU-K)	150 N m
$\eta_{MGU\text{-}K,boost}$	Efficiency (MGU-K, boost)	0.9
$\eta_{MGU\text{-}K,re}$	Efficiency (MGU-K, recuperation)	0.9
Gearbox		
i_{trans}	Transmission ratios	0.056, 0.091
n_{shift}	Shift speed	19,000 min^{-1}
e_i	Torsional mass factors	1.04, 1.04
η_g	Efficiency of gearbox and transmission	0.96
Tire		
f_{roll}	Rolling resistance	0.02
c_{tire}	Circumreference of tire	2.168 m
$p_{1,f}$	Tire model parameter	1.22 N^{-1}
$p_{2,f}$	Tire model parameter	-2.5e-5N^{-2}
$p_{1,r}$	Tire model parameter	1.42 N^{-1}
$p_{2,r}$	Tire model parameter	-2.0e-5N^{-2}

than at high speeds. To be able to apply the second and third energy management strategy, we first run one solver iteration without boosting to obtain an initial velocity profile. This profile is then used to calculate where the boost is applied for the respective strategy. Due to the mutual influence between velocity profile and boosting, a few additional iterations must be performed. The final result is found as soon as no further changes occur in the ES state at the end of the lap. This usually requires one to three iterations.

The F1 car simulated starts with 2 MJ of electrical energy in the ES and deactivated recuperation to find out how the available energy can be used most efficiently. As Table IV shows, "lowest speed" gives the best lap time and lowest fuel consumption on the Shanghai racetrack. Further simulations with other racetracks indicate that either "lowest speed" or "longest time to braking point" always results in the fastest lap time. It follows that the energy used shortly before a braking point brings very little advantage. This insight is often used in motorsports, where the drivers disengage the throttle shortly before the end of a straight and "sail" for a short time. This technique is known as "lift & coast".

D. Simulation of a Formula E car

In contrast to Formula 1 cars, Formula E cars are made up of many standard components. In the 2017/2018 season, the teams were only allowed to develop electric motors, power electronics, gearbox and rear suspension. Many of the parameters required can, therefore, be obtained from the FIA regulations [19]. Table V contains the parameters used for the simulation.

The car is simulated on the Berlin FE racetrack with a raceline length of 2,302 m. Compared to F1, the FE racetracks are shorter and narrower, as they are usually built within cities especially for this event. The calculated qualifying lap time of 69.656 s is, once again, close to the 69.620 s achieved by Lucas Di Grassi in the 2017/2018 event.

For FE teams, it is important to know how much energy a car consumes during a lap and how this changes with the application of the lift & coast technique or under yellow flag conditions. As with the yellow flags, lift & coast is integrated into the simulation via the virtual accelerator pedal. Therefore, it is set to 0% 20 m before each braking point. Under yellow flag conditions, it is set to 30%. Figures 9 and 10 show the effects of lift & coast application and yellow flag in sector 2 on velocity and ES state profiles for one lap in Berlin. With lift & coast, the lap time calculated is increased by 0.488 s. However, as can be seen in the ES state graph, applying the energy saving technique is the only way the driver can stay within the average energy available per lap. This means he has to drive many economical laps in order to be able to drive one lap at full power, for example to overtake another driver. With a yellow flag, there is much more energy left at the end of the lap.
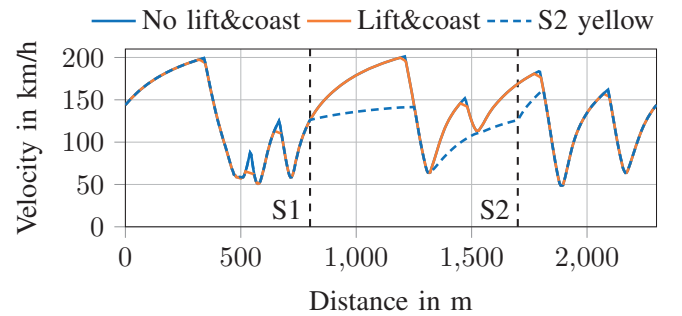

Fig. 9.   Simulated velocity profiles for a FE car on the Berlin racetrack with and without using lift & coast as well as under yellow flag conditions in sector 2. S1 and S2 are the sector boundaries.
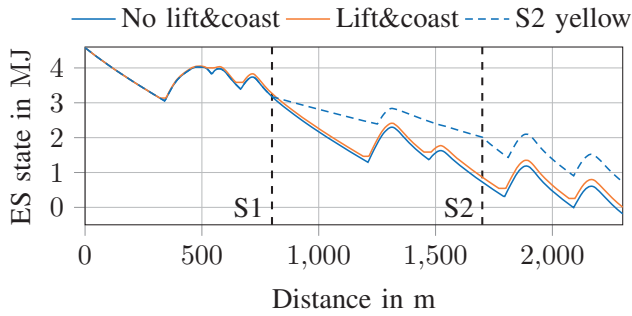
Fig. 10. Simulated ES state profiles of a FE car on the Berlin racetrack with and without using lift & coast as well as under yellow flag conditions in sector 2. The initial ES charge state was set to 4.58 MJ, which equals the energy a car has available for one lap in Berlin, on average. S1 and S2 are the sector boundaries.

V. DISCUSSION

The results show not only the functionality of our LTS, but also exemplary application cases. The LTS can be used by a race engineer to virtually optimize the vehicle setup and energy management strategy of a race car, or co-simulate a race to optimize race strategy. This option is especially suitable due to the fast computing time it enables, as well as the fact that it also allows speed limits and yellow flags to be considered. Compared to other published LTS, our proposal is easy to parametrize and has a solver that provides a good compromise between computing time and accuracy. In addition, it can easily be adapted to various racing series with different powertrain structures and topologies and includes the current state of technology. To increase model accuracy further, we would require a much more precise knowledge of vehicle parameters. Therefore, this is not suitable for our application.

There are, however, some limitations in the present state. Firstly, the tire force potential is currently assumed to be equal in longitudinal and lateral direction. This is not true for real tires. Secondly, gear changes occur infinitely fast. As a result, the model sometimes changes gears where a real driver would not. Thirdly, the modeling of MGU-K and MGU-H is kept very simple in the present state. For example, the MGU-K is only used if the torque supplied by the ICE is exhausted. In practice, it makes sense to keep the load point of the ICE in the highest efficiency range for as long as possible. As a result, the energy consumption calculation cannot be assumed to be exact. Fourthly, the maximum change in longitudinal acceleration within two consecutive segments is currently not constrained. This leads to inaccuracies in the transition points between acceleration and deceleration phases. Lastly, the energy management strategy calculations currently need a few additional solver iterations to find a valid result, due to the mutual influence between velocity profile and boosting strategy. This slightly reduces the suitability for applications with high computing time requirements.

In our future work, we will, therefore, concentrate on lifting the mentioned limitations, as well as on extending the vehicle and track library of the LTS. We also want to automate the parameter fitting process to be able to better validate the simulation models and become familiar with the error range of the simulation results. Finally, the LTS shall be used together with the mentioned race simulation to optimize race strategy.

REFERENCES

[1] M. Westerhoff, *Formula 1 Engine from Mercedes with over 50 Percent Efficiency*, https://www.springerprofessional.de/engine-technology/race-cars/formula-1-engine-from-mercedes-with-over-50-percent-efficiency/15061334, 2017, accessed: 2019-02-10.

[2] A. Heilmeier, M. Graf and M. Lienkamp, *A Race Simulation for Strategy Decisions in Circuit Motorsports*, 2018 21st International Conference on Intelligent Transportation Systems (ITSC), pp. 2986-2993, Maui, Hawaii, USA, 2018. DOI: 10.1109/ITSC.2018.8570012.

[3] B. Siegler, A. Deakin and D. Crolla, *Lap Time Simulation: Comparison of Steady State, Quasi-Static and Transient Racing Car Cornering Strategies*, SAE Technical Paper Series, no. 2000-01-3563, 2000.

[4] T. Völkl, *Erweiterte quasistatische Simulation zur Bestimmung des Einflusses transienten Fahrzeugverhaltens auf die Rundenzeit von Rennfahrzeugen*, PhD Thesis, Technical University of Darmstadt, 2013.

[5] D. Brayshaw and M. Harrison, *A quasi steady state approach to race car lap simulation in order to understand the effects of racing line and centre of gravity location*, Proceedings of the Institution of Mechanical Engineers, Part D: Journal of Automobile Engineering, vol. 219, no. 6, pp. 725-739, 2005. DOI: 10.1243/095440705X11211.

[6] I. F. Colunga and A. Bradley, *Modelling of transient cornering and suspension dynamics, and investigation into the control strategies for an ideal driver in a lap time simulator*, Proceedings of the Institution of Mechanical Engineers, Part D: Journal of Automobile Engineering, vol. 228, no. 10, pp. 1185-1199, 2014. DOI: 10.1177/0954407014525362.

[7] D. Casanova, *On Minimum Time Vehicle Manoeuvring: The Theoretical Optimal Lap*, PhD Thesis, Cranfield University, School of Mechanical Engineering, 2000.

[8] D. P. Kelly, *Lap Time Simulation with Transient Vehicle and Tyre Dynamics*, PhD Thesis, Cranfield University, School of Engineering, Automotive Studies Group, 2008.

[9] J. Timings and D. Cole, *Robust lap-time simulation*, Proceedings of the Institution of Mechanical Engineers, Part D: Journal of Automobile Engineering, vol. 228, no. 10, pp. 1200-1216, 2014. DOI: 10.1177/0954407013516102.

[10] G. Perantoni and D. J. N. Limebeer, *Optimal Control of a Formula One Car on a Three-Dimensional Track Part 1: Track Modeling and Identification*, Journal of Dynamic Systems, Measurement, and Control, vol. 137, no. 2, p. 21010, 2014. DOI: 10.1115/1.4028253.

[11] D. J. N. Limebeer and G. Perantoni, *Optimal Control of a Formula One Car on a Three-Dimensional Track Part 2: Optimal Control*, Journal of Dynamic Systems, Measurement, and Control, vol. 137, no. 5, p. 51019, 2015. DOI: 10.1115/1.4029466.

[12] D. J. N. Limebeer, G. Perantoni and A.V. Rao, *Optimal control of Formula One car energy recovery systems*, International Journal of Control, vol. 87, no. 10, pp. 2065-2080, 2014. DOI: 10.1080/00207179.2014.900705.

[13] S. Ebbesen, M. Salazar, P. Elbert, et al., *Time-optimal Control Strategies for a Hybrid Electric Race Car*, IEEE Transactions on Control Systems Technology, vol. 26, no. 1, pp. 233-247, 2018. DOI: 10.1109/TCST.2017.2661824.

[14] Roborace Ltd., *Roborace*, https://roborace.com, accessed: 2019-02-10.

[15] J. Betz, A. Wischnewski, A. Heilmeier, et al., *What can we learn from autonomous level-5 Motorsport?*, 9th International Munich Chassis Symposium 2018, Springer Vieweg, Wiesbaden, 2019. DOI: 10.1007/978-3-658-22050-1_12.

[16] OpenStreetMap Foundation, *OpenStreetMap*, https://www.openstreetmap.org, accessed: 2019-02-10.

[17] F. Braghin, F. Cheli, S. Melzi, et al., *Race Driver Model*, Computers and Structures, vol. 86, no. 13-14, pp. 1503-1516, 2008. DOI: 10.1016/j.compstruc.2007.04.028.

[18] L. Papula, *Mathematische Formelsammlung*, Springer Vieweg, Wiesbaden, 2017. DOI: 10.1007/978-3-658-16195-8.

[19] Fédération Internationale de l'Automobile, *Regulations*, https://www.fia.com/regulations, accessed: 2019-02-10.

[20] D.A.T.A.S. Ltd., *Data Analysis Tools & Simulation*, http://www.datas-ltd.com, accessed: 2019-02-10.

[21] Pirelli & C. S.p.A., *F1 and Motorsport infographics*, https://racingspot.pirelli.com/global/en-ww/infographics, accessed: 2019-02-10.